Acc. Chem. Res. **1998,** *31,* 460−466

High-Frequency EPR Spectroscopy of Large Metal Ion Clusters: From Zero Field Splitting to Quantum Tunneling of the Magnetization

ANNE-LAURE BARRA,[†] LOUIS-CLAUDE BRUNEL,[‡] DANTE GATTESCHI,*[,§] LUCA PARDI,[‡] AND ROBERTA SESSOLI[§]

Laboratoire des Champs Magnetiques Intenses, CNRS, 38042 Grenoble, France, Department of Chemistry, University of Florence, 50144 Florence, Italy, and National High Magnetic Field Laboratory, Tallahassee, Florida 32306-4005

Received May 9, 1997

Large clusters of metal ions are attracting increasing interest in several different fields.[1−4] It is well-known that small clusters of metal ions are responsible for several complex processes occurring in living organisms, and that very large clusters are present in a protein such as ferritin.[5] This has stimulated many investigations, both on simple model systems and on real biological objects. Concurrently chemistry is developing suitable strategies for the synthesis of larger and larger clusters, and recently exceptionally large rings of molybdenum ions have been obtained and fully characterized.[4]

Anne-Laure Barra was born in 1963. She received her Ph.D. in Grenoble, where she is now a research assistant at LCMI working with the high-field EPR spectrometer.

Louis-Claude Brunel received the Ph.D. in Physics from the University of Lyon in 1970. He was a scientist with the Centre National de la Recherche Scientifique in Lyon from 1971 until 1979 and was a postdoc with the University of Southern California, Los Angeles, in 1972 and 1973. In 1980 he moved to Grenoble, where he was with the High Magnetic Field Laboratory until 1994. Since March 1994 he has been Director of the EPR program at the National High Magnetic Field Laboratory, Florida State University. His scientific interests are in the development of high-field/high-frequency EPR instrumentation and methodology and their applications to the study of highly correlated electron systems.

Dante Gatteschi was born in Florence in 1945 where he graduated in 1969. He started his academic career there where he become professor of chemistry in 1980. His research interests are in magnetic molecular materials. He also has a large experience in the use of EPR spectroscopy in transition metal compounds.

Luca Pardi was born in Turin in 1957. He received a degree in chemistry at the University of Florence in 1996. He worked in Gatteschi's laboratory from 1986 to 1993 and after a short experience in France in a neutron source facility moved to Tallahassee (FL) to give his contribution to the development of the Electron Magnetic Resonance project at the National High Magnetic Field Laboratory. His main research interest is the magnetism of low-dimensional systems.

Roberta Sessoli was born in 1963 and received her Ph.D. at the University of Florence in 1992 with a thesis on molecular magnetism. Her current interests are in the investigation of the magnetic properties of large molecular clusters.

When the individual metal ions are magnetic, the clusters will in general be magnetic themselves. These clusters have many novel and interesting magnetic properties.[6−10] One of the most attractive features of molecular clusters is that they can behave as one-molecule magnets or as molecular nanomagnets.[9−12] In fact it has been possible to monitor the transition from simple paramagnetic to superparamagnetic-like behavior of the clusters.[12−14] The magnetization of the clusters at very low temperature has been observed to exchange between two possible orientations via a quantum tunneling mechanism[15,16] (QTM) and is currently under intense theoretical investigation.

Given all of these reasons of interest, it is necessary to develop suitable tools for the investigation of the magnetic properties of large clusters, to characterize the ground state and the lowest lying levels. A logical way to proceed is to measure the magnetic susceptibility and the magnetization of the clusters as a function of temperature. Although these methods are very powerful, they measure thermodynamic properties, which depend on the population of several spin levels. As such they provide indirect information, which requires the availability of a suitable model to determine the ground state. In many cases the ground state of clusters is characterized by large S values. At zero field the energy levels are split by crystal field effects, making the interpretation of the magnetization at low temperatures a difficult task.

One way to overcome this difficulty is to use a spectroscopic technique such as EPR; this technique is in principle capable of selectively detecting the response of the lowest lying levels and thereby providing direct information on them. However, the use of conventional EPR spectroscopy at 9 or 35 GHz is inconvenient because the ground state can have a large S value and a large zero field splitting, which makes the detection of the spectra either incomplete or completely impossible. In past years there has been an impressive development of spectrometers operating at high frequencies (up to 500 GHz) and consequently high fields (up to 30 T), which open new exciting possibilities for the investigation of the EPR spectra of large magnetic clusters.

In this Account we highlight the benefits of high-field (high-frequency) EPR spectroscopy, HF-EPR, for the investigation of the magnetic properties of large clusters. We will briefly recall the main instruments currently developed. We will then provide an outline of the advantages of HF-EPR spectrometers, with the main theoretical tools for spectral interpretation. Finally we will examine the experimental results, showing how HF-EPR spectroscopy has been a unique tool for obtaining information on such exotic phenomena as quantum tunneling of the magnetization in mesoscopic systems. Finally we will advocate the use of HF-EPR, not only for large clusters but more generally for the study of transition metal ion

[†] LCMI−CNRS.
[‡] NHMFL.
[§] University of Florence.

S0001-4842(96)00157-4 CCC: $15.00
Published on Web 06/13/1998

compounds which have large zero field splittings, which cannot be studied with conventional EPR techniques.

HF-EPR Spectrometers

Generally the definition of HF-EPR is EPR performed at frequencies higher than or within W-band (75−110 GHz) corresponding to resonant fields for the free electron of ca. 2.8 T and higher. HF-EPR spectrometers have been built in the past for limited purposes.[17−19] For a complete review of the subject of HF-EPR, see ref 20. One of the main technical developments that has boosted HF-EPR is the availability of superconducting magnets, although pulsed magnetic field and resistive magnets are still used.[21−23]

The existing spectrometers in the frequency range up to 150 GHz, are generally realized by extending to the high-frequency range the design of the conventional EPR spectrometers. Following the pioneering work of Lebedev[24,25] several spectrometers have been realized in this range of frequencies.[26−28] The first commercial spectrometers for continuous wave (cw) and pulsed EPR at 95 GHz and at 220 GHz were presented recently by Bruker. Most of the technological developments in HF-EPR have been tested and achieved in the 95−150 GHz range of frequencies.[27−30] Recently dielectric resonators working in the Whispering Gallery Mode have been proposed.[31]

At higher frequencies the diffraction losses increase dramatically. Even more important is the fact that the size of the single mode cavities and waveguides become too small. A quite different approach is thus needed in order to build spectrometers operating above 150 GHz. Several kinds of different sources have been used for high-frequency microwave generation depending on the application. Currently two kinds of sources are used: far infrared lasers (FIRL) and solid-state sources. The latter are in general Gunn effect diodes. CO_2 pumped FIRLs offer a series of discrete frequencies starting from ca. 160 GHz and are used in several existing EPR spectrometers operating in the millimeter and sub-millimeter range. The main disadvantage of FIRLs is their nontunability and the complexity of operation and maintenance. Gunn diodes have output power up to some tenth of a milliwatt and can be equipped with solid-state harmonic generators which multiply the fundamental frequency, and high-pass filters filter out low-frequency harmonics.

The best approach for transmitting microwaves uses quasi-optical techniques[32] in which Gaussian beams are fed into oversized waveguides, and large dielectric lenses and/or focusing mirrors are used to refocus the beam.[33] The waveguides are generally cylindrical brass pipes. Recently corrugated waveguides have been introduced to further reduce losses in transmission.[34] At Cornell University a spectrometer has been developed operating at 170 GHz and potentially in a broad band going from 100 to 300 GHz, equipped with a reflection bridge, a Fabry Perot cavity, and a novel Polarization transforming reflector which uses polarization encoding to separate the transmitted and received beams.[35] A different approach

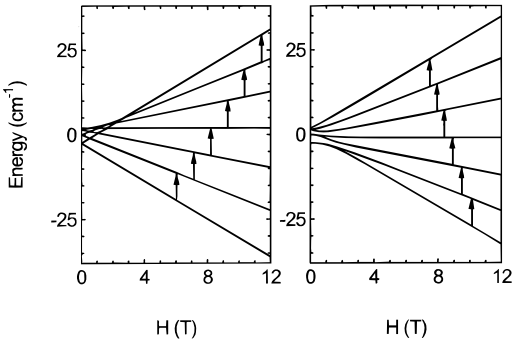

FIGURE 1. Calculated levels for $S = 3$ with $D = -0.5$ cm^{-1} and allowed EPR transitions at 245 GHz. Left: Field parallel to the unique axis. Right: Field perpendicular.

is the so-called *single pass transmission* spectrometer built in Grenoble[36,37] and at the NHMFL. These are general purpose systems offering a fairly large set of frequencies. The spectrometer implemented at the NHMFL offers a set of frequencies ranging from Q-band to 3 THz. Three different kinds of sources are used, namely, a CO_2 pumped FIRL for the high-frequency range, a set of Gunn diodes for the intermediate range (95−660 Ghz), and a millimeter network vector analyzer for the Q to D bands. The great advantage of the single pass technique resides in the very broad band of frequency that can be operated with the same experimental setting. The disadvantage is of course the reduced sensitivity which is in the range of 10^{12} spin/G at room temperature.

The detection system may be constituted by either bolometers or solid-state diodes. The helium cooled InSb detector is fast (the order of microseconds) and sensitive enough in a fairly broad frequency range from the gigahertz to the terahertz range. For faster detection Schottky diodes can be used at the expense of the sensitivity, which may fall 2 orders of magnitude.

HF-EPR Applied to Large Clusters

A system characterized by an S spin ground state can be anisotropic both in terms of g values and of crystal field (zero field splitting) effects. Of course the use of HF-EPR provides a very efficient tool for the resolution of the **g** anisotropy, because the field shifts are much larger than usually observed in low-frequency EPR. However, the main advantage of the technique is offered by the possibility of resolving the complete fine structure of the clusters, even in the presence of large zero field splittings. We document how the technique provides novel information.

In a system with $S = 3$, and axial symmetry, the energy levels can be computed with the spin Hamiltonian

$$H = \mu_B(B_z g_{\parallel} S_z + B_x g_{\perp} S_x) + D[S_z^2 - {}^1/_3 S(S+1)] \quad (1)$$

where $\parallel$ and $\perp$ refer to parallel and perpendicular to the unique axis, respectively. The energy levels are calculated within the $(2S + 1)$ functions $|S, M_S\rangle$, $-S \le M_S \le +S$. In Figure 1 we show the calculated levels for the external field parallel and perpendicular to the unique axis of the zero

field splitting tensor, respectively. For the sake of simplicity we have assumed an isotropic $g = 2$. It is apparent that if $D \gg h\nu$, where ν is the frequency of the EPR spectrometer, no allowed $\Delta M_S = \pm 1$ transition can be observed, unless one goes to extremely high fields. Therefore the use of HF-EPR can simply just show spectra which are not seen with conventional spectrometers.

The simplest case for a qualitative interpretation of the spectra is provided by the high-field limit, i.e., when $\mu_B g B_0 \gg D$. In this case $2S$ allowed $\Delta M = \pm 1$ transitions are observed; the resonance field for the $M \rightarrow M + 1$ transition is given by

$$B_r(M) = (g_e/g)[B_0 + (2M + 1)D'/2] \qquad (2)$$

where $D' = (3\cos^2\theta - 1)D/(g_e\mu_B)$, and θ is the angle of the external magnetic field with respect to the unique axis. For the external magnetic field parallel to the unique axis, the neighboring lines are separated by $2D'$, while for the external field perpendicular to the unique axis, they are separated by D'. The fine structure patterns are centered at $B = g_e B_0/g$.

An important feature of the HF-EPR spectra is that the temperature dependence of their intensity directly provides the sign of the zero field splitting parameter. In fact in a 245 GHz experiment $g\mu_B B_0$ corresponds to ca. 12 K, and the populations of the various M levels can be very different from each other. At low temperature only the lowest $M = -S$ level is populated and one transition is observed. If $D < 0$, the parallel transition is observed at low field and the perpendicular transition at high field, while the reverse is true for $D > 0$. It must be stressed that depopulation effects may start to be seen at relatively high temperatures. For instance for an $S = 3$ ground state the six allowed transitions at infinite temperature are expected to follow a relative intensity pattern 6:10:12:12:10:6, when transition probabilities are computed on the assumption of equal population of the spin levels. However, following Boltzmann statistics the same transitions, for a frequency of 245 GHz, have at room temperature a relative intensity pattern 6:9.6:11.1:10.7:8.6:5 and at 490 GHz 6:9.3:10.3:9.5:7.4:4.1.

When the Zeeman energy cannot be considered to be large compared to the zero field splitting, or when the symmetry is lower than axial, it is necessary to diagonalize the complete matrix (eq 1). Simulation procedures generally make use either of a full diagonalization combined with an interpolation technique to search for the transition fields[38−41] or of the eigenfields[42,43] and related methods[44] which directly give the transition fields. In any case the main problem, beyond the order of the matrices that need to be diagonalized, is the reconstruction of the polycrystalline powder spectrum by accumulation of single-crystal spectra.[45] The number of single-crystal spectra that need to be calculated depends on the interplay of the two main factors which determine the whole spread of the spectrum: the experimental microwave frequency and the anisotropy of the system (**g** anisotropy and ZFS). Several different strategies have been designed for that purpose[39,44−47] which are adapted to the simulation of a high-spin system with large ZFS.

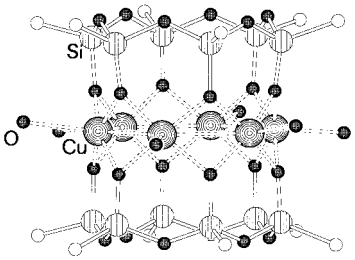

FIGURE 2. Structure of $[(PhSiO_2)_6Cu_6(O_2SiPh)_6]$, **$Cu_6$** (after ref 48). The empty unlabeled circles stay for carbon atoms.

Survey of Experimental Results

An interesting system which clearly shows the potential of the HF-EPR spectra is $[(PhSiO_2)_6Cu_6(O_2SiPh)_6]$, **$Cu_6$**, where $[PhSiO_2^-]_6$ is the hexaphenylcyclohexasiloxanolate ligand, whose structure[48] is sketched as follows:

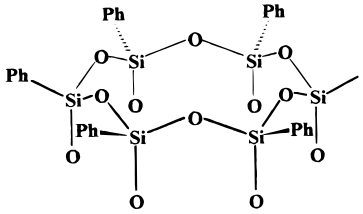

which can sandwich six metal ions to give the structure shown in Figure 2.

The magnetic properties of **Cu_6** clearly show that the coupling between the copper(II) ions is ferromagnetic, yielding a ground $S = 3$ state.[49] X-band EPR spectra show three features in the 0−0.6 T region, which agree with a ground $S = 3$ state. In particular there is a transition observed close to zero field which suggests that there is a pair of levels which are separated by about 0.3 cm^{-1}, but no conclusion concerning the nature of the ground state can be reached without elaborate fitting strategies.

The polycrystalline powder HF-EPR spectra recorded at 245 GHz provide a much more convincing picture of the ground-state multiplet. In fact in this case the Zeeman energy is ca. 8 cm^{-1}, which is much larger than D. Therefore the spectra show the regular features of Figure 3, which to a good approximation correspond to the high-field limit of the spectra. In the spectra obtained at 20 K, at least five perpendicular features, separated by ca. 0.28 T are clearly observed, confirming the ground $S = 3$ state and the zero field splitting $D' = 0.28$ T. The increase of the intensity of the lowest field perpendicular feature at ca. 7.2 T on decreasing temperature is dramatic, as can be seen by the comparison of the spectra at 100 and 5 K, respectively. Therefore, the zero field splitting parameter is unambiguously seen to be positive.

The use of HF-EPR spectroscopy in this case was essentially confirmatory, but in other cases HF-EPR was decisive in the assignment of the correct ground state of the cluster. $[Mn_{10}O_4(biphen)_4X_{12}]^{4-}$ **Mn_{10}**, where X = Cl, Br, biphen = 2,2′-biphenoxide, has the structure[50] shown

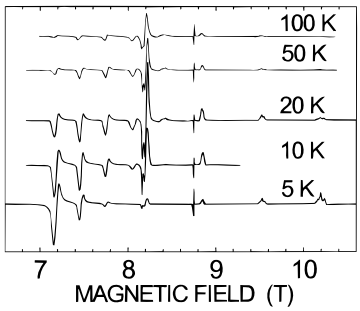

FIGURE 3. Polycrystalline powder HF-EPR spectra of **Cu_6** at 245 GHz (after ref 49). The narrow signal at ca. 8.75 T is from the standard (dpph).

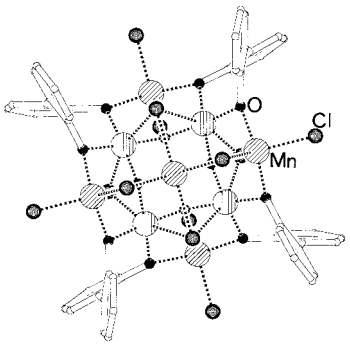

FIGURE 4. Structure of $[Mn_{10}O_4(biphen)_4Cl_{12}]^{4-}$ **Mn_{10}**, viewed along the S_4 axis (after ref 50). The large circles are manganese ions. The ones with vertical lines inside are Mn^{3+}.

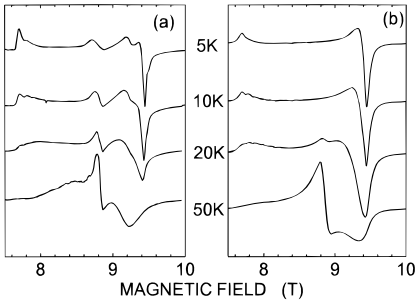

FIGURE 5. HF-EPR spectra at 245 GHz of a polycrystalline sample of **Mn_{10}** pressed in a pellet: (a) experimental; (b) calculated for $S = 12$ and $D = -0.047$ cm^{-1} (after ref 51).

in Figure 4. It is comprised of four manganese(III) ions, with $S = 2$, and six manganese(II) ions, with $S = {}^5/_2$, arranged in a complex three-dimensional structure determined by the presence of four μ_4-oxo groups. The analysis of the magnetic properties suggests that the ground state is $S \geq 12$, but no unambiguous conclusion could be reached because of the presence of a moderate zero field splitting which makes the analysis difficult. The 9 GHz EPR spectra of **Mn_{10}** are rather uninformative, with many broad features between 0 and 1 T, and sharper ones which cannot be interpreted. The polycrystalline powder spectra recorded at 245 GHz are shown[51] in Figure 5. On lowering the temperature the spectra acquire intensity at the extreme fields. In particular the low-field feature is a parallel transition, indicative of a negative zfs. A satisfactory simulation of the spectra could be achieved by setting $S = 12$, $g_{\parallel} = 1.974$, $g_{\perp} = 1.983$, $D = -0.047$ cm^{-1}. Attempts to use different S values only lead to worse fitting of the

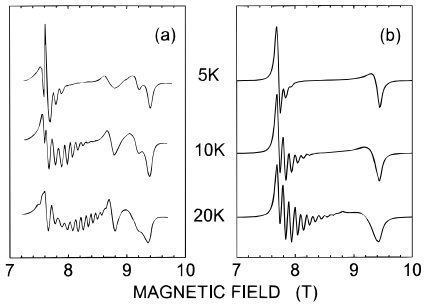

FIGURE 6. Loose polycrystalline powder HF-EPR spectra of **Mn_{10}** at 245 GHz: (a) experimental; (b) calculated for $S = 12$ and $D = -0.047$ cm^{-1} with partial orientation of the powder (after ref 51).

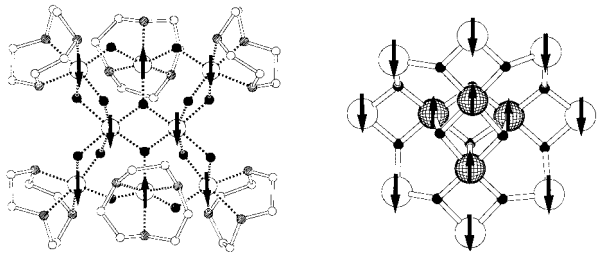

FIGURE 7. Structures of **$Mn_{12}Ac$** (left) and **Fe_8** (right) and suggested spin orientation in the ground state. For **$Mn_{12}Ac$** only the $Mn_{12}O_{12}$ core is reported for the sake of clarity.

spectra. Therefore the HF-EPR spectra unambiguously show that the ground state of **Mn_{10}** is $S = 12$.

Another important feature of the HF-EPR spectra is that the crystallites tend to orient in the strong field needed for the measurements. To avoid this, the crystallites were pressed into a pellet. However, it may be convenient to leave the crystallites free to orient, thus recording pseudo single crystal spectra. This is shown in Figure 6: by comparison with Figure 5 one can see that orientation has been achieved. At least 12 equally spaced features in the low-field region have been observed, and the spectra on the right have been calculated by assuming the same parameters as above with a Gaussian distribution of crystallites on the possible orientations in the static magnetic field. We estimate that under these conditions ca. 90% of the crystallites have the z axis to within 3° of the field direction.

The accurate knowledge of the spin Hamiltonian parameters of these clusters, and especially of the zero field splitting is not just a curiosity for EPR spectroscopists, but it provides unique information on the barrier for the reorientation of the magnetization of the cluster at low temperature and for quantum tunneling of the magnetization. These data are not yet available for **Mn_{10}**; however, they are available for two other clusters, namely, $[Mn_{12}O_{12}(CH_3COO)_{16}]$, **$Mn_{12}Ac$**,[52] and $[(tacn)_6Fe_8O_2(OH)_{12}]^{8+}$, **$Fe_8$**,[53] whose structures are shown in Figure 7 where tacn is triazacyclononane. Both compounds have a ground $S = 10$ state.[54,55] **$Mn_{12}Ac$** comprises an external ring of eight manganese(III) ions, each with $S = 2$, and an internal tetrahedron of four manganese(IV) ions, each with $S = {}^3/_2$, while **Fe_8** has only iron(III) ions, each with $S = {}^5/_2$. The ground $S = 10$ states can be justified with the spin distribution of Figure 7.

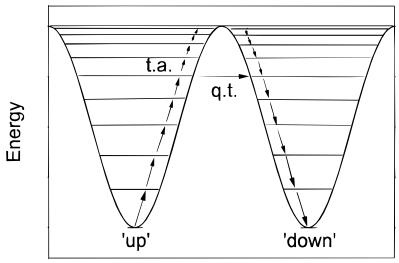

FIGURE 8. Energy barrier for the reorientation of the magnetization in spin systems with $S = 10$ and negative zero field splitting. Thermally activated (ta) and quantum tunneling (qt) processes are schematized by the arrows.

The HF-EPR spectra of both compounds have been of paramount importance for determining the nature of the ground states and the zero field splitting. In fact initially the ground state of **Fe_8** was described as either $S = 9$ or $S = 10$ on the basis of magnetization measurements at low temperature.[55] **$Mn_{12}Ac$** has an axial zero field splitting, while that of **Fe_8** is rhombic. Early experiments on **$Mn_{12}Ac$** performed with loose polycrystalline powders showed only one feature at low temperature, corresponding to oriented crystallites. They yielded $D = -0.5$ cm^{-1}. Accurate spectra recorded for **Fe_8** gave $D = -0.2$ cm^{-1}, $E/D = 0.16$.

In the context of Figure 8, when the temperature is sufficiently low only the lowest $M = \pm 10$ levels are populated. If the cluster is in the $M = -10$ state, the magnetization is up, while if it is in the $M = +10$ state, the magnetization is down (up/down meaning the magnetization has the direction/the opposite direction of the external magnetic field). The mechanism of relaxation of the magnetization can be depicted as shown in Figure 8. In the absence of an external magnetic field the magnetization can be either up or down, and the two potential energy wells are identical. In quantum mechanical language the system can be either in the $M = -10$ or $M = +10$ energy level with the same probability. To invert the magnetization, it is necessary that a spin passes from, say, $M = -10$ to $M = +10$. This must be done in steps, changing M by ± 1. Therefore the spin system must climb all of the ladder of levels from $M = -10$ to $M = -9$, then to $M = -8\cdots$ up to $M = 0$, and then descend, one step at a time to $M = +10$. According to the Hamiltonian (1) the barrier corresponds to $\Delta = DS^2 = 100$ D in the present case.

The zero field splitting data of **$Mn_{12}Ac$** and **Fe_8** therefore showed that the barrier for reorientation of the magnetization in the ground state is $\Delta/k \approx 70$ K for the former and $\Delta/k \approx 28$ K for the latter. Consequently slow relaxation effects can be anticipated at low temperature. The relaxation time of the magnetization is found to follow a thermally activated law:

$$\tau = \tau_0 \exp(\Delta/kT) \tag{3}$$

$\tau_0 = 2.1 \times 10^{-7}$ s, $\Delta/k = 62$ K for **$Mn_{12}Ac$** and $\tau_0 = 1.9 \times 10^{-7}$ s, $\Delta/k = 22$ K for Fe_8. This behavior is the same as that observed in superparamagnets, i.e., bulk magnetically ordered systems in which, due to the small size of the particles, the reorientation of the magnetization follows the thermally activated law of eq 3. Therefore at low temperature these clusters behave like single-molecule magnets.[12]

The thermally activated process can occur by absorbing and emitting phonons. This process is analogous to the Orbach process of relaxation of paramagnets.[56] It was found[57] that at low temperature the relaxation time is given by:

$$\tau = C\frac{S^6}{\Delta^3}\exp(\Delta/kT) \tag{4}$$

where C is a constant which depends on the phonon coupling and on Δ. The important result is that the relaxation time follows a thermally activated process, with a preexponential factor which depends on S^6. This justifies why slow relaxation effects are observed in systems with large spins, such as the ones described here.

At lower temperatures the relaxation times become so long that an alternative mechanism of relaxation of the magnetization may become competitive. In fact at 2 K **$Mn_{12}Ac$** has a relaxation time of the order of 2 months. Under these conditions quantum tunneling of the magnetization can become a valid alternative to the thermally activated process.[58]

The best evidence reached so far of quantum tunneling of the magnetization has been achieved through the measurement[15,16] of the hysteresis loop of **$Mn_{12}Ac$**. To observe tunneling, the spin Hamiltonian should include a term that does not commute with S_z, which corresponds to a transverse magnetic anisotropy.[58] In **$Mn_{12}Ac$** the symmetry is axial; therefore only fourth order terms of the crystal field can introduce the required anisotropy. These terms have long been used in EPR for spin systems with $S \geq 2$.[59] The corresponding spin Hamiltonian has the form

$$H = B_4^0 O_4^0 + B_4^4 O_4^4 \tag{5}$$

where B_4^0 and B_4^4 are parameters and $O_4^0 = 35S_z^4 - 30S(S+1)S_z^2 + 25S_z^2 - 6S(S+1) + 3S^2(S+1)^2$ and $O_4^4 = {}^1/_2(S_+^4 + S_-^4)$. The latter is the term responsible of the transverse anisotropy.

The inclusion of (5) in the spin Hamiltonian produces clear changes in the EPR spectra. Both B_4^0 and B_4^4 are in general much smaller than D, because they produce a perturbation on the levels determined by the second-order zero field splitting terms. In qualitative terms the inclusion of the quartic terms makes the pattern of transitions irregular also when the Zeeman term is much larger than the crystal field terms. To reach this condition, we recorded[60] the spectra of **$Mn_{12}Ac$** at 525 GHz, shown in Figure 9. At this frequency the resonant field of the free electron is 18.73 T. Therefore a hybrid (resistive + superconducting) magnet was needed in order to record the spectra. The lowest "parallel" transition was observed at 8.03 T and the highest "perpendicular" transition at 24.2 T. Under these conditions the spectra should conform to the high-field approximation of eq 2, but the separations between the parallel and perpendicular lines are not

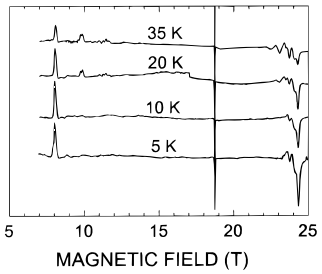

FIGURE 9. Polycrystalline powder HF-EPR spectra of **$Mn_{12}Ac$** at 525 GHz (after ref 60). The narrow signal at ca. 17.8 T is from the standard (dpph).

regular, showing that the fourth-order terms must be included. Analogous spectra were recorded at lower frequencies. From all of these data it was possible to obtain a more accurate set of parameters, $D = -0.46$ cm^{-1}, $B_4^0 = -2.2 \times 10^{-5}$ cm^{-1}, and $B_4^4 = \pm 4 \times 10^{-5}$ cm^{-1}. Therefore HF-EPR provided for the first time an experimental parameter to feed into the theoretical models for QTM.

Conclusions

The examples we have worked out here are, in a sense, extreme examples to show the utility of HF-EPR spectroscopy in large magnetic clusters. However the field which this work is opening is an extremely interesting one, even for simple compounds. For the first time it has in fact become possible to obtain spectra of ions such as iron(II), manganese(III), chromium(II), and nickel(II) which have not been investigated so far due to the large zero field splitting. Recently porphirine[61] and β-diketonate[62] manganese(III) complexes have been investigated with HF-EPR spectroscopy, and the spin Hamiltonian parameters have been precisely determined. The fact that some of these ions are involved in metalloproteins and metalloenzymes makes the use of HF-EPR even more attractive.

Also clusters such as those of iron−sulfur proteins or of photosystem II can be profitably investigated through HF-EPR spectroscopy in order to have access to states which up to now have been EPR silent or did not provide all of the experimental data which are needed in order to work out suitable models of the structure. Even ferritin can in principle be investigated through this technique.

The authors are pleased to acknoweledge the improvements in the manuscript by B. Robinson. The financial support of Italian MURST and CNR is gratefully acknowledged as well as the support received by the European TMR program under Contract No. ERBFMGECT950077.

References

(1) Hagen, K. S. *Angew. Chem., Int. Ed. Engl.* **1992**, *31*, 1036.
(2) Lippard, S. J. *Angew. Chem., Int. Ed. Engl.* **1988**, *27*, 353.
(3) Müller, A.; Pope, M. T. *Polyoxometalates: From Platonic Solids to Antiretroviral Activity*; Kluwer: Dordrecht, The Netherlands, 1994.
(4) Müller, A.; Krickemeyer, E.; Meyer, J.; Bögge, H.; Peters, F.; Plass, W.; Diemann, E.; Dillinger, S.; Nonnebruch, F.; Randerath, M.; Menke, C. *Angew. Chem., Int. Ed. Engl.* **1995**, *34*, 2122.
(5) Harrison, P. M.; Artymyuk, P. J.; Ford, G. C.; Lawson, D. M.; Smith, J. M. A.; Treffry, A.; White, J. L. In *Biomineralization*; Mann, S., Webb, J., Williams, R. J. P., Eds.; VCH: Weinheim, Germany, 1989; p 257.
(6) Gatteschi, D.; Caneschi, A.; Cornia, A.; Sessoli, R. *Chem. Soc. Rev.* **1996**, 101.
(7) Taft, K. L.; Papaefthymiou, G. C.; Lippard, S. J. *Science* **1993**, *259*, 1302.
(8) Gider, S.; Awschalom, D. P.; Douglas, T.; Mann, S.; Chaparala, M. *Science* **1995**, *268*, 77.
(9) Gatteschi, D.; Caneschi, A.; Pardi, L.; Sessoli, R. *Science* **1994**, *265*, 1054.
(10) Eppley, H. J.; Tsai, H.-L.; de Vries, N.; Folting, K.; Christou, G.; Hendrickson, D. N. *J. Am. Chem. Soc.* **1995**, *117*, 301.
(11) Scuiller, A.; Mallah, T.; Nivorozkhin, A.; Verdaguer, M.; Veillet, P. *New J. Chem.* **1996**, *20*, 1−3.
(12) Sessoli, R.; Gatteschi, D.; Caneschi, A.; Novak, M. A. *Nature* **1993**, *365*, 141.
(13) Barra, A.-L.; Debrunner, P.; Gatteschi, D.; Schulz, C. E.; Sessoli, R. *Europhys Lett.* **1996**, *35*, 133.
(14) Papaefthymiou, G. C. *Phys. Rev. B* **1992,** *46*, 366.
(15) Friedman, J. R.; Sarachick, M. P.; Tejada, J.; Maciejewski, J.; Ziolo, R. *Phys. Rev. Lett.* **1996**, *76*, 3830.
(16) Thomas, L.; Lionti, F.; Ballou, R.; Gatteschi, D.; Sessoli, R.; Barbara, B. *Nature* **1996**, *383*, 145.
(17) Alpert, Y.; Couder, Y.; Tuchendler, J.; Thome, H. *Biochim. Biophys. Acta* **1973**, *322*, 34.
(18) Date, M. *J. Phys. Soc. Jpn.* **1975**, *39*, 892.
(19) Magarino, J.; Tuchendler, J.; D'Haenens, J. P. *Phys. Rev.* B **1975**, *14*, 865. (b) van Blockstal, L.; Herlach, F. *J. Phys. Condens. Matter* **1990,** *2*, 7187.
(20) Eaton, S. S.; Eaton, R. G. *Magn. Reson. Rev.* **1993**, *16*, 157.
(21) Muller, F.; Huant, S.; Karrai, K.; Dampne, G.; Grynberg, M.; Martinez, G.; Brunel, L. C. *J. Phys. C* **1987**, *7*, 717.
(22) Palme, W.; Ambert, G.; Boucher J. P.; Dhalenne, G.; Revcolevschi, A. *Phys. Rev.* **1996**, *76*, 4817.
(23) Motokawa, M. In *High Field Magnetism*; Date, M., Ed.; North-Holland: Amsterdam, 1983.
(24) Lebedev, Y. *Russ. Chem. Rev.* **1983**, *52*, 850.
(25) Lebedev, Y. *Appl. Magn. Reson.* **1995**, *7*, 339.
(26) Prisner, T. F.; van der Est, A.; Bittl, R.; Lubitz, W.; Stehlik, D.; Möbius, K. *Chem. Phys.* **1995**, *194*, 361.
(27) Weber, R. T.; Disselhorst, A. J. M.; Prevo, L. J.; Schmidt, J.; Weckenbach, W. Th. *J. Magn. Reson.* **1989**, *81*, 129.
(28) Haindl, E.; Möbius, K.; Oloff, H. *Z. Naturforsh.* **1984**, *40a*, 169.
(29) Amity, H. J. *Rev. Sci. Instrum.* **1970**, *41*, 1492.
(30) Prisner, T. F.; Un, S.; Griffin, R. G. *Isr. J. Chem.* **1992**, *32*, 357.
(31) Colligiani, A.; Longo, I.; Martinelli, M.; Lucchesi, M.; Pardi, L. *Appl. Magn. Reson.* **1996**, *9*, 567.
(32) Lebedev, Y. In *Modern Pulsed and Continuous Wave ESR*; Kevan, L., Bowman, M. K., Eds.; Wiley: New York, 1990.
(33) Selected papers on: *Gaussian Beam Mode Optics for Millimeter-Wave and Terahertz Systems*; Lesurf, J. C. G., Ed.; SPIE Optical Engineering Press: Bellingham, WA, 1993.
(34) Freed, J. In *Advanced EPR Application in Biology and Biochemistry*; Hoff, A. J., Ed.; Elsevier: Amsterdam, 1989.
(35) Earle, K. A.; Tipikin, D. S.; Freed, J. H. *Rev. Sci. Instrum.* **1996**, *67*, 2302.

(36) Barra, A.-L.; Brunel, L. C.; Robert, J. B. *Chem. Phys. Lett.* **1990**, *165*, 107.
(37) Muller, F.; Hopkins, M. A.; Coron, N.; Grynberg, M.; Brunel, L. C.; Martinez, G. *Rev. Sci. Intrum.* **1989**, *60*, 3681.
(38) Mabbs, F. E.; Collison, D. *Electron Paramagnetic Resonance of d Transition Metal Compounds*; Elsevier: Amsterdam, London, New York, Tokyo, 1992.
(39) Mombourquette, M. J.; Weil, J. A. *J. Magn. Reson.* **1992**, *99*, 37.
(40) Jacobsen, C. J. H.; Pedersen, E.; Viladsen, J.; Weihe, H. *Inorg. Chem.* **1993**, *32*, 1216.
(41) Bencini, A.; Gatteschi, D. In *Transition Metal Chemistry;* Nelson, G. A., Figgis, B. M., Eds.; Dekker: New York, 1982; Vol. 8.
(42) Belford, G. G.; Belford, R. L.; Burkhalter, J. F. *J. Magn. Reson.* **1973**, *11*, 251.
(43) Bencini, A.; Uytterhoeven, M Unpublished results.
(44) Cugunov, L.; Mednis, A.; Kliava, J. *J. Magn. Reson. A* **1994**, *106*, 153.
(45) Wang, D.; Hanson, G. R. *J. Magn. Reson.* **1995**, *117*, 1.
(46) Gribnau, M. C. M.; van Tits, J. L.; Reijerse, E. J. *J. Magn. Reson.* **1990**, *90*, 474.
(47) Pilbrow, J. R. *Appl. Magn. Reson.* **1996**, *10*, 45.
(48) Igonin, V. A.; Shchegolikhina, O. I.; Lindeman, S. V.; Levitsky, M. M.; Struchkov, Yu. T.; Zhdanov, A. A. *J. Organomet. Chem.* **1992**, *423*, 351.
(49) Rentschler, E.; Gatteschi, D.; Cornia, A.; Fabretti, A. C.; Barra, A.-L.; Shchegolikhina, O. I.; Zhdanov, A. A. *Inorg. Chem.* **1996**, *35*, 4427.
(50) Goldberg, D. P.; Caneschi, A.; Delfs, C. D.; Sessoli, R.; Lippard, S. J. *J. Am Chem. Soc.* **1995**, *117*, 5789.
(51) Barra, A.-L.; Caneschi, A.; Gatteschi, D.; Sessoli, R. *J. Am. Chem. Soc.* **1995**, *117*, 8855.
(52) Lis, T. *Acta Crystallogr., Sect. B* **1980**, *36*, 2042.
(53) Wieghardt, K.; Pohl, K.; Jibril, I.; Huttner, G. *Angew. Chem., Int. Ed. Engl.* **1984**, *23*, 77.
(54) Caneschi, A.; Gatteschi, D.; Sessoli, R.; Barra, A.-L.; Brunel, L.-C.; Guillot, M. *J. Am. Chem. Soc.* **1991**, *113*, 5873.
(55) Delfs, C.; Gatteschi, D.; Pardi, L.; Sessoli, R.; Wieghardt, K.; Hanke, D. *Inorg. Chem.* **1993**, *32*, 3099.
(56) Orbach, R. *Proc. R. Soc. London, Ser. A* **1961**, *264*, 458.
(57) Villain, J.; Hartman-Boutron, F.; Sessoli, R.; Rettori, A. *Europhys. Lett.* **1994**, *27*, 159.
(58) Novak, M. A.; Sessoli, R. In *Quantum Tunneling of the Magnetization*; Gunther, L.; Barbara, B., Eds.; NATO ASI Series E, Vol. 301; Kluwer: Dordrecht, The Netherlands, 1995.
(59) Abragam, A.; Bleaney, B. *Electron Paramagnetic Resonance of Transition Ions*; Dover: New York, 1986.
(60) Barra, A. L.; Gatteschi, D.; Sessoli, R. *Phys. Rev. B* **1997**, *56*, 8192.
(61) Goldberg, D. P.; Telser, J.; Krzystek, J.; Montalban, A. G.; Brunel, L. C.; Barrett, A. G. M.; Hoffman, B. M. *J. Am. Chem. Soc.* **1997**, *119*, 8722.
(62) Barra, A. L.; Gatteschi, D.; Sessoli, R.; Abbati, G. L.; Cornia, A.; Fabretti, C. A.; Uytterhoeven, M. G. *Angew. Chem., Int. Ed. Engl.* **1997**, *109*, 22309.

AR960157P